International Journal of Current Research and Modern Education (IJCRME)
ISSN (Online): 2455 - 5428
(www.rdmodernresearch.com) Volume I, Issue I, 2016

SYNTHESIS AND CHARACTERIZATION OF $Cd_{0.9-x}Zn_{0.1}Cu_xS$ BY CO-PRECIPITATION TECHNIQUE

C. Sathiyapriya*, S. Rajivgandhi, A. Ravikumar** & A. Dinesh Kumar*****

* PG Scholar, Department of Physics, Srinivasan College of Arts and Science, Perambalur, Tamilnadu

** Assistant Professor, Department of Physics, Dhanalakshmi Srinivasan Engineering College, Perambalur, Tamilnadu

*** Assistant Professor, Department of Mathematics, Dhanalakshmi Srinivasan Engineering College, Perambalur, Tamilnadu

Abstract:

The Cd0.9-xZn0.1CuxS composite were synthesized by co precipitation method with various combinations. Nano particles on the samples are confirmed by X-ray Diffraction analysis. The size of the grains and micro strains are calculated by using XRD technique. Furthermore the prepared samples were characterized by Scanning Electron Microscope (SEM) with Energy dispersive X-ray EDX and Fourier Transform Infra-Red Spectroscopy (FTIR). Results from the characterizations are tabulated and shown.

1. Introduction:

Nanotechnology is a continuation of miniaturization from micron meter scale down to nanometer scale. Materials in this size range exhibit some different physical properties. For example, crystal in the nanometer scale have a low melting point and reduced lattice constant, since the number of surface atoms or ions becomes a significant fraction of the total number of atoms or ions and the surface energy plays a significant role in the thermal stability. Nanostructure materials can be made with unique nanostructures and properties. This field is expected to open new venues in science and technology. The discovery of novel materials, process, and phenomena at the nano scale, as well as the development of new experimental and theoretical techniques for research provide fresh opportunities for the development of innovative nano system and nano structured system. Nanosystems are expected to find various unique properties and applications. It is expected to open new venues in science and technology.

2. Experimental Techniques:

Cadmium doped ZnO nano particles were synthesized by co-precipitation technique.

2.1. Preparation of $Cd_{0.9-x}Zn_{0.1}Cu_xS$ (x = 0, 0.02, 0.04, 0.06) Nanoclusters:

$Cd_{0.9-x}Zn_{0.1}Cu_xS$ (x = 0, 0.02, 0.04, 0.06) nanoclusters were prepared by simple chemical co-precipitation method using cadmium acetate dihydrate ($Cd(CH_3COOH)_2{\cdot}2H_2O$), zinc acetate dihydrate ($Zn(CH_3COO)_2.2H_2O$), copper acetate dihydrate ($Cu(CH_3COOH)_2{\cdot}2H_2O$) and sodium sulfide ($Na_2S$) as the precursors. The high purity AR grade chemicals such as ($Cd(CH_3COOH)_2{\cdot}2H_2O$), ($Zn(CH_3COO)_2.2H_2O$), ($Cu(CH_3COOH)_2{\cdot}2H_2O$) and Na_2S purchased from Merck chemical Co. were used as source materials of Cd^{2+}, Zn^{2+} , Cu^{2+} and S^{2-} ions, respectively without further purification.

For the preparation of $Cd_{0.88}Zn_{0.1}Cu_{0.02}S$ nanoclusters, 0.88M cadmium acetate dihydrate, 0.1 M zinc acetate dihydrate and 0.02 M copper acetate dihydrate were slowly dissolved (one by one) in 50 ml double distilled water and kept at constant stirring for 30 min to get clear and homogeneous solution. A separate solution was prepared by dissolving 1 M sodium sulfide in 50 ml double distilled water. The

preparation process is based on the slow release of Cd^{2+}, Zn^{2+}, Cu^{2+} and S^{2-} ions in the solution. The ions condense on an ion-ion basis in the solution. The prepared solution was added drop wise to the initial solution under constant stirring at room temperature. The desired pH value, 9.5 was achieved by the addition of aqueous ammonia solution proportionally into the mixture of chemicals. To ensure the proper reaction, the final solution was stirred continuously for 2 h at room temperature. A brownness precipitate was filtered and then washed several times using double distilled water and ethanol to eliminate the impurities and acetate ions from the precipitates. The collected precipitates were dried using an oven at 100˚C for 18 h. The precipitates were collected and grounded using an agate mortar. The same procedure was repeated for the remaining samples synthesized with nominal compositions of $Cd_{0.9-x}Zn_{0.1}Cu_xS$ (x = 0, 0.02, 0.04, 0.06) nanoclusters. The color of the nanoclusters was changed from golden yellow to brown depending on Cu concentrations from 0% to 6%.

The above nanoparticles were characterized by using X-ray diffraction (XRD), Scanning Electron Microscopy (SEM), optical absorption spectroscopy, optical transmission spectroscopy and Fourier Transform Infra-Red Techniques (FTIR).

3. Result and Discussion:

3.1. X-Ray Diffraction (XRD)—Structural Study:

XRD is one of the important tools to analyze the structure of the crystalline material. In order to determine the crystal structure of Zn-doped CdS and Zn, Cu co-doped CdS nanoclusters with different Cu concentration between 2% and 6%, XRD patterns were taken from 20° to 60° and shown in Figure 1. $Cd_{0.9}Zn_{0.1}S$ nanoclusters exhibit three major diffraction peaks corresponding to the diffraction angles 27.15˚ (111), 44.47˚ (220), and 52.32˚ (311) with preferred orientation along (111) plane. The standard diffraction peaks exhibited by the nanoclusters are matched with the JCPDS card no.40- 454 having a cubic zinc blende structure which is in good agreement with the reported data on CdS system [1-3]. The similar result was observed by Dutkova et al. and reported that $Cd_{1-x}Zn_xS$ nanoclusters exhibited a phase transition from hexagonal to cubic with an increase of Zn content [4]. It is evident from the XRD spectra that there are no extra peaks corresponding to Cd, Zn, and Cu oxides or sulfide of Cd, Zn, Cu or related secondary and impurity phases. Thus, XRD confirms the phase singularity of the synthesized material, which also confirms the formation of Cd-Zn-Cu-S alloy nanoclusters rather than separate nucleation or phase formation. The observed identical diffraction of all Cu doped compounds confirms the structure of the compound is not altered due to the inclusion of Cu ion.

Compared to Zn-doped CdS sample, Cu doped $Cd_{0.9}Zn_{0.1}S$ sample has relatively lower diffracted intensity along (111) plane which indicates that Cu^{2+} ions are doped in to Cd–Zn–S lattice successfully. The average crystallite size (D) of the nanoclusters is calculated after appropriate background correction from X-ray line broadening of the diffraction peaks of (111) plane using Debye- Scherrer's formula [5],

$$\text{Average crystallite size (D)} = \frac{0.9\,\lambda}{\beta \cos\theta}$$

Where λ is the wave length of X-ray used (1.5408Å), β is the angular peak width at half maximum in radian along (111) plane, and θ is the Bragg's diffraction angle. The micro-strain (ε) developed in the nanoclusters are calculated using the formula [6].

$$\text{Micro-strain} = \frac{\beta \cos\theta}{4}$$

Where λ is the wavelength of X-ray used (Å), β is the angular peak width at half maximum in radian, and θ is the Bragg's diffraction angle.

Table-1 shows the peak position (2θ), full width at half maximum (FWHM, β) value, d-value, cell parameter 'a', average crystallite size (D) and micro-strain (ε) of $Cd_{0.9-x}Zn_{0.1}Cu_xS$ nanoclusters for different Cu concentrations from 0% to 6%. It is noticed from table 1 that as the amount of Cu dopant increased, the peak at (111) seemed to be shifted towards higher 2θ. This was due to the formation of hexagonal phase as mentioned above. Since the cubic (111) and the hexagonal (002) lines coincide, it is very difficult to differentiate the cubic from the hexagonal structure [7]. The lattice parameter of Cu-doped $Cd_{0.9}Zn_{0.1}S$ is always greater than $Cd_{0.9}Zn_{0.1}S$. As the ionic radius of Cu^{2+} (0.73Å) is smaller than that of Cd^{2+} (0.97Å), it can easily enter in to the crystal lattice of CdS and occupy the substitution sites. The insertion of Cu^{2+} brings the distortion in Cd-Zn-S lattice which made the lattice parameter of Cu-doped $Cd_{0.9}Zn_{0.1}S$ is always higher than $Cd_{0.9}Zn_{0.1}S$. In addition, it is expected that Cu ions not only substitute Cd ions but occupy some interstitial lattice sites in Cd-Zn-S.

The average crystallite size is reduced from 2.10 nm to 2.02 nm by Cu doping from 0% to 6%. It is concluded from table 1 that the change in crystallite size of $Cd_{0.9}Zn_{0.1}Cu_xS$ solid solution particles does not change significantly with the Cu concentration. Moreover, the micro-strain of $Cd_{0.9-x}Zn_{0.1}Cu_xS$ nanoclusters is increased when Cu-doping is increased from 2% to 6%. The increase of strain causes the decrease of lattice parameters and average crystallite size. This increase of micro-strain is responsible for the broadening of diffraction peaks [8]. The peak position (2θ value), FWHM value, d-value, cell parameter 'a', average crystallite size (D) and micro-strain (ε) of $Cd_{0.9-x}Zn_{0.1}Cu_xS$ (x = 0, 0.02, 0.04, 0.06) nanoclusters at room temperature.

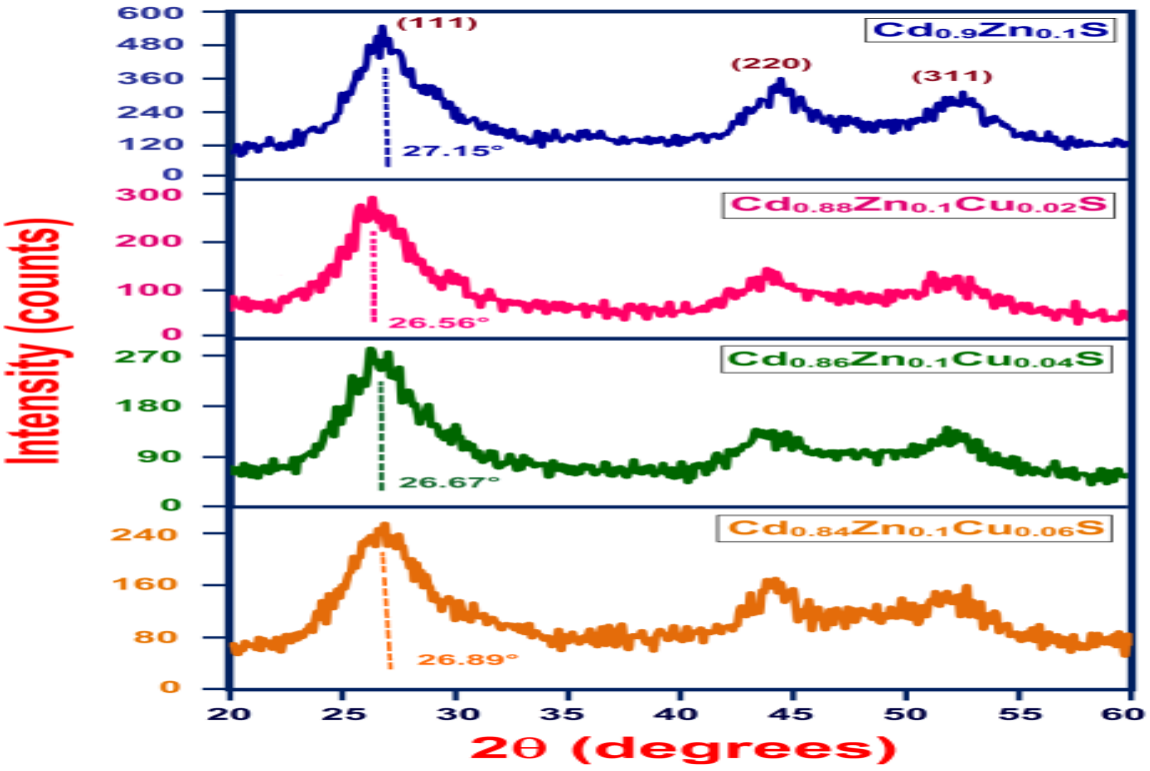

Figure 1: X-ray diffraction pattern of $Cd_{0.9-x}Zn_{0.1}Cu_xS$ nanoclusters with x = 0%, 2%, 4% and 6% from 20° to 60°

Table – 1

Samples	Peak position 2θ (˚)	FWHM (β) (degrees)	d value (Å)	Cell parameter a = b = c (Å)	Average Crystallite size (D) (nm)	Micro-strain (ε)(10^{-3}
$Cd_{0.9}Zn_{0.1}S$	27.15	3.89	3.281	5.683	2.10	16.503
$Cd_{0.88}Zn_{0.1}Cu_{0.02}S$	26.56	3.59	3.355	5.810	2.16	16.020
$Cd_{0.86}Zn_{0.1}Cu_{0.04}S$	26.67	3.82	3.337	5.780	2.14	16.204
$Cd_{0.84}Zn_{0.1}Cu_{0.06}S$	26.89	4.03	3.318	5.746	2.02	17.118

3.2. Scanning Electron Microscope (SEM): Surface Characteristics:

In order to determine the morphology, size and shape of the grains and growth mechanism, typical scanning electron microscopy measurements were carried. The entire samples exhibit the agglomerated grains in the cluster. Figure 2a shows the SEM micrograph of $Cd_{0.9}Zn_{0.1}S$ nanoclusters. Spherically shaped granules structure are seen in the form of clusters in undoped $Cd_{0.9}Zn_{0.1}S$ sample, which are not distributed uniformly and the sample shows amorphous nature. Figure 2b shows the surface morphology of Cu = 2% doped sample. The surface morphology undergoes a change when Cu is added to the reaction solution. As the reaction proceeds some of these particles are stabilized to form further increase of Cu decreases the grain size. Figure 2c shows the SEM image of Cu = 4% doped sample. Addition of cu modifies its surface which shows compact distribution over the surface and good connectivity between defined grains. It is clearly noticed from Figure 2d that the average grain size is decreased by Cu- doping as noticed in Table-1. At higher Cu concentrations (Cu = 6%) grains are agglomerated on the surface which suggest that the growth process starts with the colloidal nano-clusters.

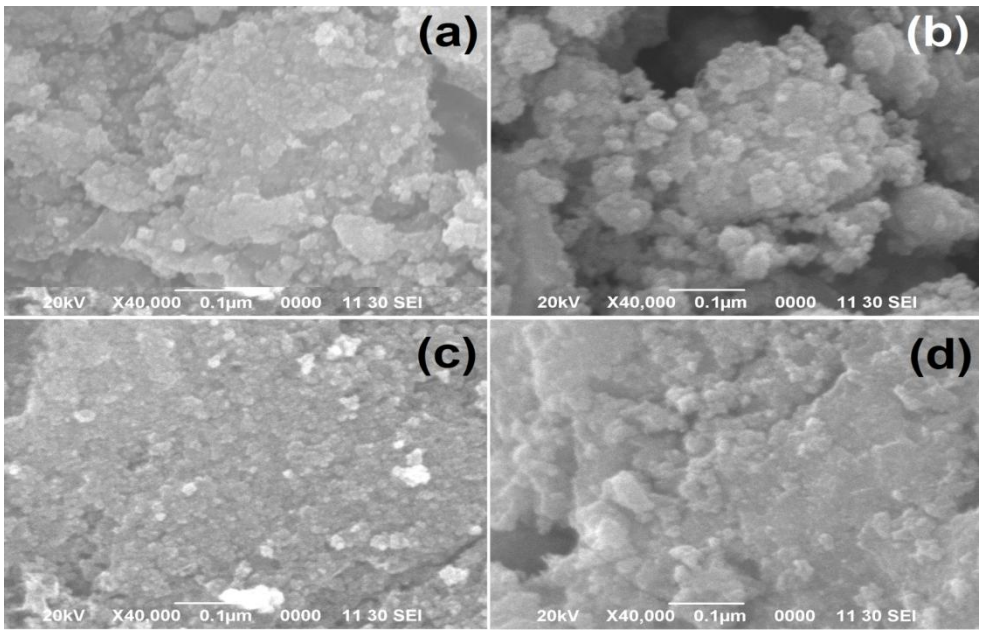

Figure 2: SEM Images of (a) $Cd_{0.9}Zn_{0.1}S$, (b) $Cd_{0.88}Zn_{0.1}Cu_{0.02}S$, (c) $Cd_{0.86}Zn_{0.1}Cu_{0.04}S$ and (d) $Cd_{0.84}Zn_{0.1}Cu_{0.06}S$ Nanoclusters

3.3 Energy Dispersive X-ray (EDX) Spectra: Compositional Analysis:

Figure 3 shows the typical EDX spectra of $Cd_{0.9}Zn_{0.1}S$, $Cd_{0.88}Zn_{0.1}Cu_{0.02}S$, $Cd_{0.86}Zn_{0.1}Cu_{0.04}S$ and $Cd_{0.84}Zn_{0.1}Cu_{0.06}S$ nanoclusters. The defined peaks corresponding to Cd, Zn, Cu and S confirmed that stoichiometry of the constituent is maintained in the finally prepared compounds and the numerical are given in Table 2. The quantitative atomic percentage of the compositional elements such as Cd, S, Zn and Cu in $Cd_{0.9}Zn_{0.1}S$, $Cd_{0.88}Zn_{0.1}Cu_{0.02}S$, $Cd_{0.86}Zn_{0.1}Cu_{0.04}S$ and $Cd_{0.84}Zn_{0.1}Cu_{0.06}S$ nanoclusters are presented in Table 2.

Atomic percentage of Cd is periodically decreased when Cu doping percentage is increased from 0% to 6%. It appears that the Cd rich ions are replaced by Cu ions in the Cd-Zn-Cu-S lattice. Table 2 shows that the Cu/ (Cd+Zn+Cu) ratio is 2.21%, 4.02% and 6.28% for Cu = 2%, 4% and 6%, respectively which is very close to their nominal stoichiometry within the experimental error. The observed slight fluctuation in the atomic percent values from table 2 may be due to the small region of the sample has been taken for recording the EDX spectra.

Table – 2

The quantitative analysis of atomic percentage of the compositional elements presents in $Cd_{0.9-x}Zn_{0.1}Cu_xS$ (x = 0, 0.02, 0.04, 0.06) nanoclusters using EDX analysis.

Samples	Atomic percentage of the elements (%)				Cu/(Cd+Zn+Cu) ratio (%)
	Cd	S	Cu	Zn	
$Cd_{0.9}Zn_{0.1}S$	53.02	41.36	-	5.62	-
$Cd_{0.88}Zn_{0.1}Cu_{0.02}S$	52.23	40.87	1.31	5.59	2.21
$Cd_{0.86}Zn_{0.1}Cu_{0.04}S$	50.98	41.02	2.37	5.63	4.02
$Cd_{0.84}Zn_{0.1}Cu_{0.06}S$	49.74	40.95	3.71	5.60	6.28

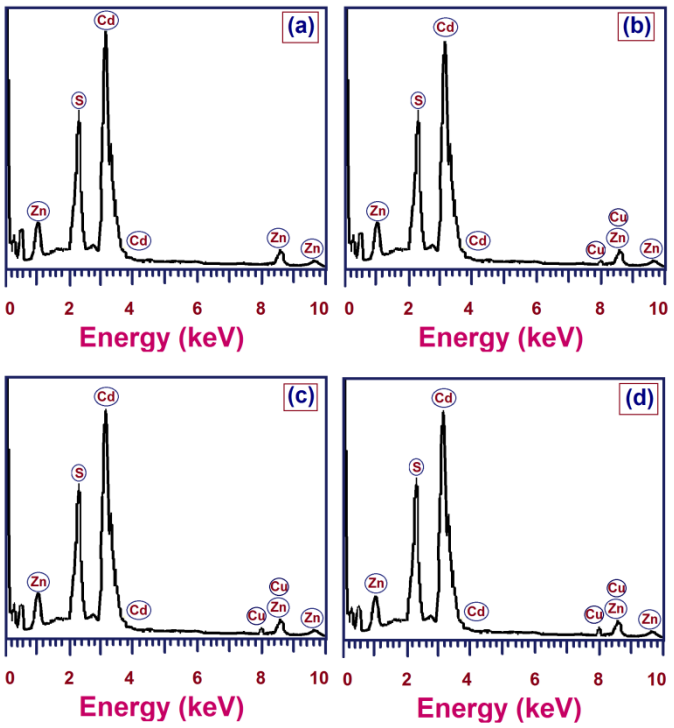

Figure 3: Energy dispersive X-ray (EDX) spectra of (a) $Cd_{0.9}Zn_{0.1}S$, (b) $Cd_{0.88}Zn_{0.1}Cu_{0.02}S$, (c) $Cd_{0.86}Zn_{0.1}Cu_{0.04}S$ and (d) $Cd_{0.84}Zn_{0.1}Cu_{0.06}S$ Nanoclusters

3.3. Fourier Transforms Infrared (FTIR) Studies:

FTIR is one of the best techniques used to get the information about the chemical bonding present in the material. It is used to identify and characterize the organic species / elemental constituting in the material. The characteristic peaks exhibited by FTIR spectra of $Cd_{0.9-x}Zn_{0.1}Cu_xS$ nanoclusters recorded in the wavelength range 400-4000 cm^{-1} are as shown in Figure 4a. The IR frequencies along with the vibrational assignments of the nanoclusters assigned at room temperature are listed in Table 2.

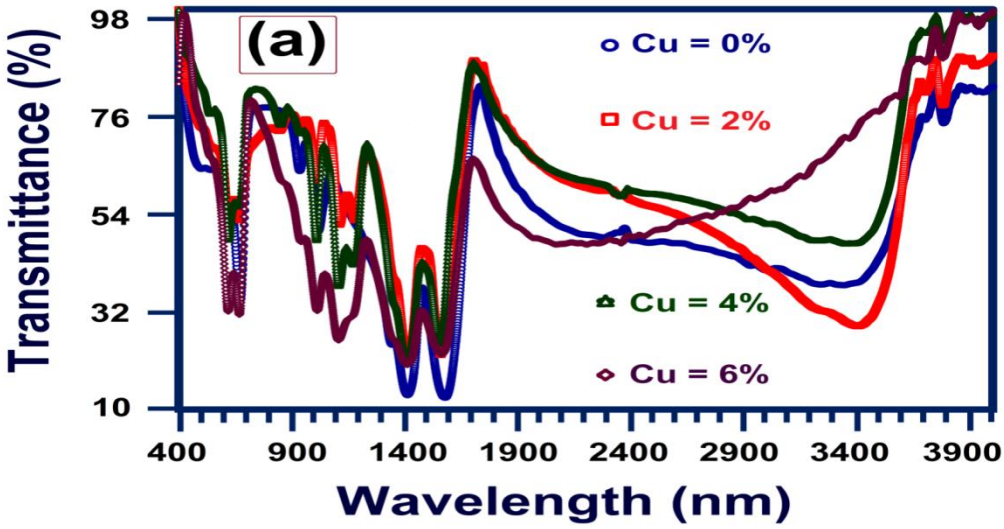

Figure 4: (a) FTIR spectra of $Cd_{0.9-x}Zn_{0.1}Cu_xS$ nanoclusters with different Cu concentrations from 0% to 6% at room temperature in the wave number from 400 to 4000 cm^{-1},

Figure 4: (b) The enlarged FTIR spectra in the wave number range 400 cm^{-1} – 1000 cm^{-1}.

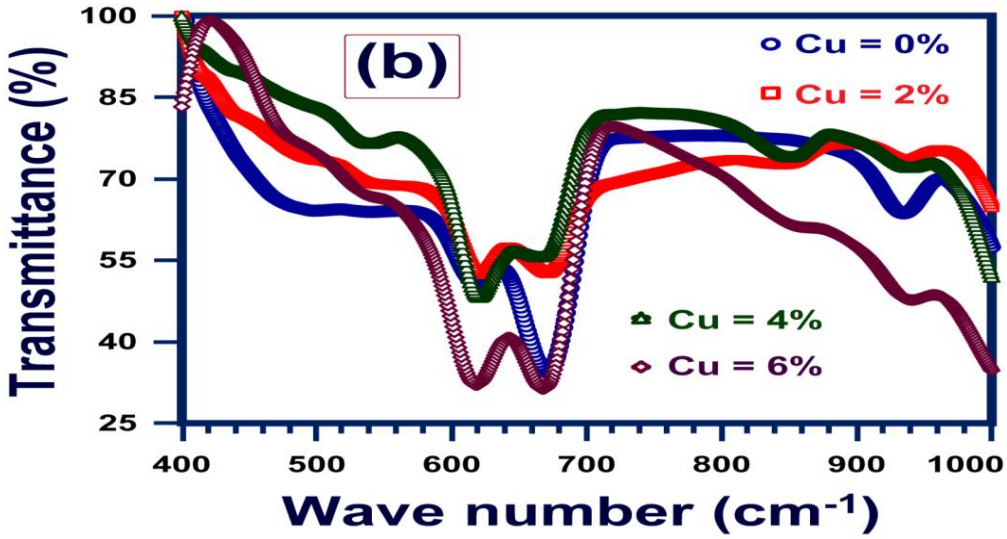

The broad absorption band at near 3200–3700 cm^{-1} is due to the presence of O–H stretching vibrations of water (H_2O) molecules [9]. The band at 2375 cm^{-1} is due to the C=O stretching modes arising from the absorption of atmospheric CO_2 on the surface of the particles [10]. Another peak at1405 cm^{-1} suggests the involved C–H bending [11]. A small and weak band around 1610 cm^{-1} is due to the H–O–H bending vibration of the

water molecules [12]. There are doublet medium asymmetric stretching bonds C–O observed at 1129 cm^{-1} and 1267 cm^{-1} these bonds may be due to the environmental and / or chemical impurities that are always present [13].

Figure 4b shows the enlarged FTIR spectra of $Cd_{0.9-x}Zn_{0.1}Cu_xS$ nanoclusters between the 400 cm^{-1} and 4000 cm^{-1}. The vibration absorption peaks observed at 821 cm^{-1} and 732 cm^{-1} are assigned to Cd–S stretching [14, 15]. The absorption peaks at 621 cm^{-1} is assigned to Zn–S stretching [16]. In our case, for Zn = 10% doped CdS absorption peaks at 618 cm^{-1} and 678 cm^{-1} are assigned to Cd-Zn–S stretching vibration. When Cu is introduced, stretching of Cd-Zn-Cu-S bond is assigned to 677 cm^{-1} (Cu = 2%) which is shifted to lower wave number side as 675 cm^{-1} for $Cd_{0.86}Zn_{0.1}Cu_{0.04}S$; 671 cm^{-1} for $Cd_{0.84}Zn_{0.1}Cu_{0.06}S$. The observed shift in the frequency of the present system is due to the presence of Cu in Cd–Zn–S lattice and also the size effect.

Table - 3

IR peaks and their assignments of undoped $Cd_{0.9-x}Zn_{0.1}Cu_xS$ (x = 0, 0.02, 0.04, 0.06) nanoclusters at room temperature.

Assignments	Wave number (cm^{-1})			
	$Cd_{0.9}Zn_{0.1}S$	$Cd_{0.88}Zn_{0.1}Cu_{0.02}S$	$Cd_{0.86}Zn_{0.1}Cu_{0.04}S$	$Cd_{0.84}Zn_{0.1}Cu_{0.06}S$
O-H stretching vibration of H_2O	3338	3402	3351	3400
C=O stretching vibration due Co_2	2375	2371	2376	2374
H-O-H bending vibration of H_2O	1621	1610	1625	1631
C–H bending	1405	1408	1406	1405
C–O asymmetric stretching bonds	1129	1128	1115	1122
	1267	1261	1266	1269
Stretching mode of Cd-Zn-S	618	618	621	625
(doublet)	678	677	675	671

4. Conclusions:

$Cd_{0.9-x}Zn_{0.1}Cu_xS$ ($0 \le x \le 0.06$) nanoclusters were successfully synthesized by a conventional chemical co-precipitation method at room temperature. XRD confirms the phase singularity of the synthesized material, which also confirmed the formation of Cd-Zn-Cu-S alloy nanoclusters rather than separate nucleation or phase formation. Atomic percentage of Cd is periodically decreased when Cu doping percentage is increased from 0% to 6%. It appears that the Cd rich ions are replaced by Cu ions in the Cd-Zn-Cu-S lattice. When Cu is introduced, stretching of Cd-Zn-Cu-S bond is shifted lower wave number side from 678 cm^{-1} (Cu = 0%) to 671 cm^{-1} (Cu = 6%) due to the presence of Cu in Cd–Zn–S lattice and also the size effect.

5. References:

1. R. Mariappan, V. Ponnuswamy, M. Ragavendar, D. Krishnamoorthi, C. Sankar, The effect of annealing temperature on structural and optical properties of undoped and Cu doped CdS thin films, OPTIK , 123 (2012) 1098.

2. Sedaghat Z, Tagavinia N, Marandi M (2006) Thermal control of the size and crystalline phase of CdS nanoparticles. Nanotechnology 17: 3812–3814.
3. Simmons, B.A.; Li, S.; John, V.T.; McPherson, G.L.; Bose, A.; Zhou, W.; He, J. Morphology of CdS nanocrystals synthesized in a mixed surfactant system. Nano Lett 2002, 2, 263–268.
4. E. Dutkova, P. Balaz, P. Pourghahramani, A. V. Nguyen, V. Sepelak, A. Feldhoff, J.
5. Kovac, A. Satka, Mechanochemical solid state synthesis and characterization of CdxZn1-xS nanocrystals, Solid State Ionics179 (2008) 1242.
6. S. Muthukumaran, R. Gopalakrishnan, Structural, optical and photoluminescence properties of Zn 1−x Ce x O (x = 0, 0.05 and 0.1) nanoparticles by sol–gel method annealed under Ar atmosphere, J. Sol–Gel Sci. Technol.62 (2012)193.
7. P.P. Hankare, P.A. Chate, D.J. Sathe, P.A. Chavan, V.M. Bhuse, Effect of thermal annealing on properties of zinc selenide thin films deposited by chemical bath deposition, J. Mater. Sci. Mater. Electron. 20 (2009) 374.
8. S. Sain, S.K. Pradhan, Mechanochemical solid state synthesis of $(Cd_{0.8}Zn_{0.2})S$ quantum dots: Microstructure and optical characterizations,J. Alloys Compd. 509 (2011) 4176–4184.
9. J. Pelleg, E. Elish, Stress changes in chemical vapor deposition tungsten silicide(polycide)film measured by x-raydiffraction, J. Vac. Sci. Technol. A 20 (2002) 754.
10. Z. R. Khan, M. Zulfequar, M.S. Khan, Optical and structural properties of thermally evaporated cadmium sulphide thin films on silicon (1 0 0) wafers,Mater. Sci. Eng. B 174 (2010) 145–149.
11. S. B. Quadri, E.F. Skelton, D. Hsu, A.D. Dinsmore, J. Yang, H.F. Gray, B.R. Ratna, Size-induced transition-temperature reduction in nanoparticles of ZnS,Phys. Rev. B 60 (1999) 9191–9193.
12. N. R. Pavaskar, C.A. Menezes, A.B.P. Sinha, J. Electrochemical Society 124 (1977) 743–748.
13. B. Malinowska, M. Rakib, G. Durand, Analytical characterization of cadmium cyanamide in CdS thin films and bulk precipitates produced from CBD process in pilot plant, Solar Energy Mater. Solar Cells 86 (2005) 399.
14. G. Yellaiah, K. Hadasa, M. Nagabhushanam, Growth, characterization, optical and vibrational properties of Sm^{3+} doped $Cd_{0.8}Zn_{0.2}S$ semiconductor compounds, J. Crys. Growth 386 (2014) 62–68.
15. V. Singh, P. Chauhan, Structural and optical characterization of CdS nanoparticles prepared by chemical precipitation method., J. Phys. Chem. Solids70 (2009) 1074–1079.
16. P. Kumar, N. Saxena, F. Singh, A. Agarwal, Nanotwinning in CdS quantum dots, Physica B 407 (2012) 3347–3351.
17. B.S. Remadevi, R. Raveendran, A.V. Vaidyan, Synthesis and characterization of Mn^{2+}-doped ZnS nanoparticles, Pramana – J. Phys. 68 (2007) 679–687.